

INTRINSIC FORMING OF HYBRID PARTS MADE OF LASER-STRUCTURED ALUMINIUM SHEET AND CFRP PREPREG

S. Wu¹, J. Freund², A. Delp³, J. Haubrich², M. Löbbbecke², F. Walther³ and T. Tröster¹

¹ Paderborn University, Chair of Automotive Lightweight Design, Mersinweg 7, 33100 Paderborn, Germany

² German Aerospace Center (DLR), Institute of Materials Research, Linder Hoehe, 51147 Cologne, Germany

³ TU Dortmund University, Chair of Materials Test Engineering (WPT), Baroperstr. 303, 44227 Dortmund, Germany

¹ shuang.wu@upb.de,

² Jonathan.Freund@dlr.de,

³ alexander.delp@tu-dortmund.de,

Keywords: Hybrid parts, combined forming, laser structuring, adhesion properties

ABSTRACT

This paper introduces an intrinsic manufacturing process of a hat profile made of laser-pretreated aluminium sheet of alloy EN AW-6082 in T6 condition and carbon fibre-reinforced plastic (CFRP) prepreg. The resin system used in combination with CFRP was epoxy resin (EP). Before manufacturing, the laser-pretreated aluminium sheet and CFRP prepreg were stacked to form a multi-layer composite, which was pressed simultaneously in one process step. The optimal CFRP layer structure was calculated in advance using the finite element method. During the forming process, the curing reaction and the joining of the aluminium sheet and CFRP prepreg will take place simultaneously. Thus, further joining techniques such as bonding and riveting could be saved, and a much more efficient process could be achieved. After manufacturing, shear-edge test was used to characterize the adhesion properties of the hybrid part.

1 INTRODUCTION

Today's societal constraints, such as adherence to legal CO₂ restrictions, consumer comfort standards, and an acute range problem for electric vehicles, force the automobile industry to develop its cars more lightly [1]. For example, the European Commission revised the CO₂ targets for new passenger cars and vans in July 2021. The proposed regulation would require a reduction in CO₂ emissions from passenger cars of 55% by 2030, as opposed to the former regulations of 37.5% [2]. There are various methods to reduce vehicle weight. One way is to use light metals and fibre-reinforced plastics, which are often found in high-class vehicle bodies with low and medium production quantities, for example, the Mercedes AMG GT. In contrast, high-tensile steels are often used in vehicles with high-volume mass production, such as Volkswagen Golf [1]. Due to the ease of integration into existing processes of steel materials, more and more research has been conducted in recent years to develop new types of steel materials. For example, Tata Steel has developed lightweight steel, especially for chassis, which combines high strength and good formability [3]. However, the lightweight design trend for mass-produced automobiles is now led by multi-material design. By combining multiple materials, such as aluminium reinforced with carbon fibre-reinforced plastics (CFRP), components can be improved to meet various criteria such as mechanical properties, manufacturability and costs. This way, the gaps between structures made of light metals and fibre-reinforced plastics in small to medium series and lightweight steel in large series can be bridged [1].

2 STATE OF THE ART

In multi-material design, the adhesion between the different materials strongly influences the component properties [4]. There are various ways to bond metal and fibre-reinforced plastics, such as adhesive bonding, clinching, riveting or screwing. However, additional weight by necessary overlaps

and fasteners or material damage cannot be avoided so that the full lightweight potential of multi-material design cannot be completely exhausted [5]. On the other hand, it could be more efficient to produce hybrid components using the so-called intrinsic process. Intrinsic means that the curing of the resin system and the joining process of different materials take place simultaneously during the forming process, so no further assembly is necessary after the manufacturing process [6].

The current research also tends towards the intrinsic production of hybrid components to save process time and enable mass production of hybrid parts. Much research has already focused on fibre-reinforced thermoplastics, as they are easy to recycle and only need a short manufacturing time [7]. For example, Behrens has successfully produced a hat profile consisting of aluminium sheets and glass fibre-reinforced thermoplastics in one process step [8]. The aluminium sheet was first stacked with glass-fibre-reinforced thermoplastics to form a sandwich composite, which was formed together in the next step. Here, the thermoplastics melted at an elevated process temperature serve directly as an adhesive to avoid an additional bonding process. Furthermore, David Trudel-Boucher compares the mechanical properties of a hybrid U-profile made of steel and fibre-reinforced thermoplastics (FRTP), joined with two technologies. One uses a metal sheet with hooks on the metal surface to achieve mechanical interlocking with the molten plastics. The other is adding additional adhesive film to increase the bond strength. This way, a hybrid U-profile could be formed in one process step with both technologies. The results have shown that the U-profiles with mechanical interlocking can achieve higher force at failure and absorb higher energy [9]. Nevertheless, each material has its advantages and disadvantages. Applying a bonding agent is often necessary to improve the joining properties of hybrid parts with FRTP [10]. Especially with Polypropylene (PP), it is impossible to bond without an adhesion promoter or pre-treatment due to its low polarity and surface energy [11, 12].

Compared to thermoplastics, thermosets are characterized by their better adhesiveness. Furthermore, thanks to their lower viscosity at room temperature, thermosets can impregnate the fibres better and energy-efficiently [13]. Therefore, developing hybrid components with fibre-reinforced thermoset plastics is also very important. For example, Wang has investigated manufacturing a hat profile consisting of steel and CFRP using the Resin Transfer Molding (RTM) process. The steel sheet was formed first, followed by preforming of the CFRP scrim. After inserting the formed steel sheet and the CFRP preform into the preheated mould, epoxy resin injection occurs. Then, under heat and pressure, the curing of epoxy resin and the bond to the metal sheet co-occurred [5]. Moreover, the prepreg pressing process is particularly suitable for producing hybrid components due to the high degree of automation and high component quality [14]. For example, Lauter has developed a double Z-profile consisting of a DD11 steel sheet reinforced with CFRP prepreg based on epoxy resin [15]. However, the steel sheet was formed first, and the CFRP-prepreg was pressed into the metal structure in the next step, which caused additional process effort. Hybrid parts consisting of metal and fibre-reinforced thermosets could be successfully produced using the two manufacturing processes mentioned above. In addition, better crash properties were achieved compared to mere steel construction. Nevertheless, the shaping of the metal sheet and fibre-reinforced plastics did not occur simultaneously as in the other processes with thermoplastics, which leads to additional process steps. Therefore, a new pressing process for the intrinsic production of hybrid components consisting of aluminium sheet and CFRP based on epoxy resin was developed and investigated within the scope of this work.

3 EXPERIMENTAL BASIS

3.1 Materials

For manufacturing the hybrid hat profile, sheets of the aluminium alloy EN-AW 6082 in T6 condition with 2 mm thickness and unidirectional CFRP prepreg from SGL Carbon were used. It was delivered on a roll and covered with a release film. The fibre volume content is 61 %. Prepregs are pre-impregnated continuous fibres with high viscosity matrix, characterized by their easy handling, good mechanical properties, and closely tolerable fibre matrix ratio. Due to the reactive matrix, they often have to be stored below -18°C [14].

3.2 Design of the hat profile

To ensure that the CFRP layer structure of the hat profile is load-optimised, a Finite Element (FE) calculation was first carried out to determine the optimum layer structure. Figure 1 shows the dimension of the hat profile. The CFRP part consists of 8 individual prepreg layers, with a total thickness of approximately 2.5 mm in the uncured state.

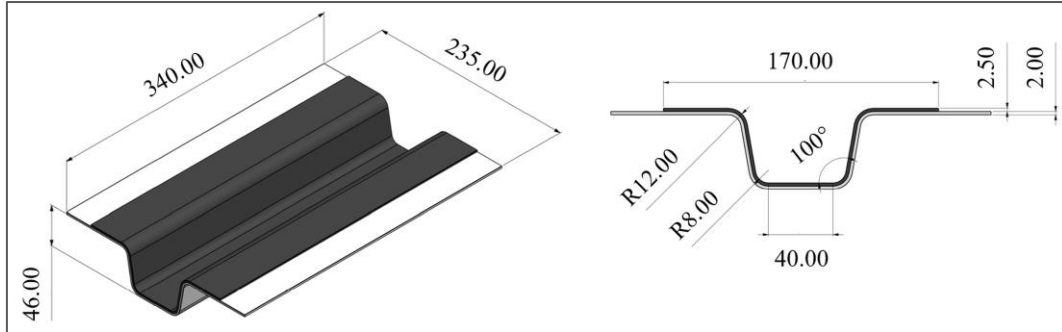


Figure 1: Dimension of the hat profile

The Abaqus software was used to determine the optimal CFRP layer structure. For this purpose, only the CFRP part was considered and simulated under flexural load, similar to an actual load case. The simulation setup is shown in Figure 2, where the three cylinders are assumed to be rigid. The upper cylinder acts downwards with a force of 1000 N, while the movement of the lower supports is locked in all three directions. According to Hooke's law, the smaller the displacement of an object at a constant force, the greater the stiffness [16]. Therefore, the displacement in the middle of the hat profile was defined as a criterion to find the optimal layer structure.

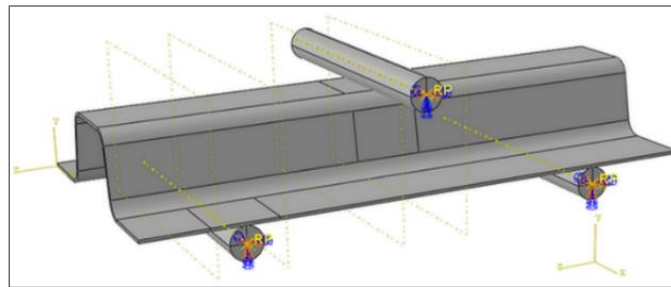


Figure 2: Simulation setup to determine the load-optimized CFRP layer structure

Due to the anisotropy, carbon fibres have significantly better mechanical properties in the fibre direction, so the fibre direction should be along the profile length as far as possible. However, the carbon fibres of the CFRP prepreg are not sewn together as in a multiaxial scrim, so the individual not yet cured prepreg layer can be squeezed to the sides due to the high forming force. For this reason, the fibre direction of the first and last layer was aligned along the flow direction of the forming process, referred to as 0° in the following. Figure 3a shows an initial layer structure in which the fibre direction of all layers is at 0° .

The fibre direction for the other layer structures could vary by 45° from layer 2 to 6. Then, with the help of the Isight software, 4096 combinations could be generated and imported into Abaqus to calculate the displacement under the defined bending load in the next step. The simulation results have shown that the displacement is 0.5866 mm for the initial layer structure, which is the worst and can be attributed

to the fibre direction being transverse to the profile length. The lowest displacement was found at the layer structure shown in Figure 3b, 0.3201 mm. From ply 1 to 8, the fibre direction is $0^\circ/45^\circ/-45^\circ/90^\circ/90^\circ/45^\circ/-45^\circ/0^\circ$.

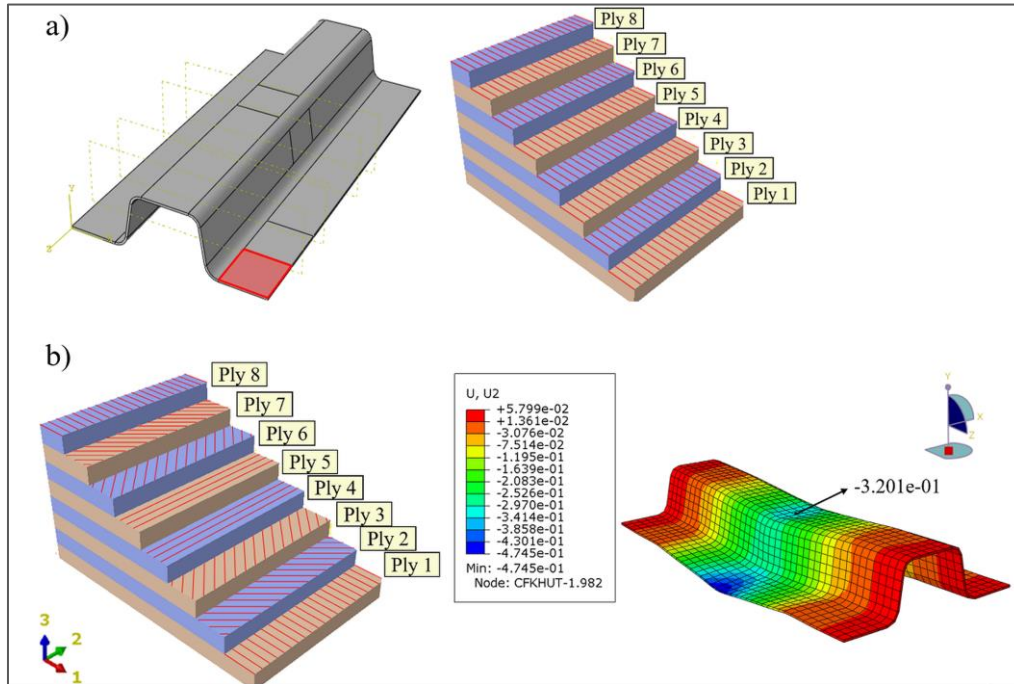


Figure 3: a) Illustration of the initial layer structure, all layers are at 0° , b) the optimal layer structure and its displacement under flexural load

3.3 Manufacturing parameters

The epoxy resin system serves as an adhesive in intrinsic manufacturing, so sufficient curing after the manufacturing process is necessary. Therefore, the influence of consolidation parameters (temperature, time, pressure) on the mechanical properties was investigated in advance on plate samples. Finally, a promising parameter combination can be concluded: process temperature 150°C , production time 5 min, pressing pressure 0.5 MPa. The curing force of the hat profile could then be calculated according to equation 1, using the projected area of CFRP prepreg (see Figure 1).

$$(170 \text{ mm} * 340 \text{ mm} * 0.5 \text{ MPa}) / 1000 = 28.9 \text{ kN} = \text{approx. } 30 \text{ kN} \quad (1)$$

In the separate forming process, the metal sheet is often formed first. Then the FRP part is pressed into the formed metal structure and cured. In this case, the pressing force is only used to cure the resin system. In contrast, with intrinsic production, the component has a complex stress state during the combined forming process, which should be investigated more closely in further research. Moreover, additional force is required to form the metal sheet. From preliminary tests, a force of approx. 90 kN was measured, which is necessary to form the aluminium sheet. Therefore, the value calculated according to (1) is only the force necessary to cure the CFRP. The pressing force should be greater to hold the aluminium sheet in the correct position after forming. Therefore, the pressing force was set at 120 kN, which results from the pure forming (90 kN) and curing force (30 kN). Furthermore, another force value, 130 kN, was also chosen to investigate the influence of the pressing force on the component properties.

As mentioned above, the aluminium surface was laser structured to improve the adhesion properties of the hybrid parts. The laser pre-treatment was carried out at the Institute of Materials Research, German Aerospace Center in Cologne, using a pulsed Nd: YAG CleanLaser CL20 (Clean Lasersysteme

GmbH, Herzogenrath, Germany) with a wavelength of 1064 nm, an average pulse length of 110 ns and a duty cycle of 40 %. Subsequently, Single-Lap-Joint samples were produced with the same epoxy resin used in the CFRP prepreg, and the adhesion properties were investigated. Finally, three optimal laser parameters were found to increase the bond strength significantly. (Table 1)

Parameter number	Frequency (kHz)	Power (W)	Overlap of laserspots (%)	Number of scans
P1	60	20	10	5
P2	40	20	50	1
P3	60	15	50	1

Table 1: Parameter of laser pre-treatment

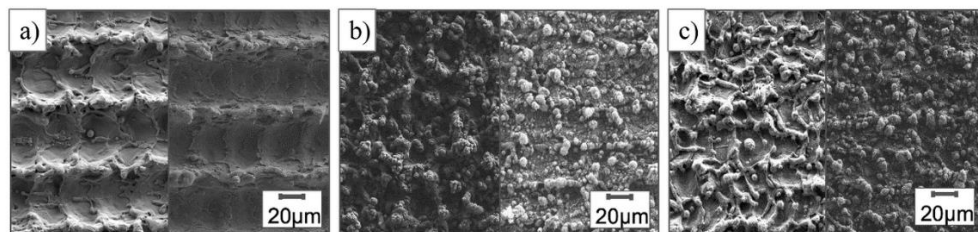


Figure 4: Scanning electron microscope (SEM) recordings of the surface structure of laser parameters, a) P1, b) P2, c) P3

Furthermore, laser parameter 1 showed an utterly different microstructure compared to the other laser parameters (Figure 4). It can be seen from Figure 4 that laser parameter 1 has a direction-dependent structure. Moreover, it is also proven by a roughness measurement that the pretreated surface has a significantly higher roughness, which is also dependent on the laser direction [17]. Therefore, the laser direction of laser parameter 1 was also observed during manufacturing. Table 2 lists all parameter combinations.

Manufacturing parameter	Laser parameter		Specimen name
150°C, 120 kN, 5 min	P1	Direction 1	120_P1_D1
	P1	Direction 2	120_P1_D2
	P2	-	120_P2
	P3	-	120_P3
150°C, 130 kN, 5 min	P1	Direction 1	130_P1_D1
	P1	Direction 2	130_P1_D2
	P2	-	130_P2
	P3	-	130_P3

Table 2: List of parameter combinations to produce the hybrid hat profile

3.4 Development of the pressing tool

A pressing tool was developed to produce the hybrid hat profile, shown in Fig. 5. The production takes place on a servo-motorised spindle press from Synchropress GmbH, Germany. Heating cartridges

(1000 W and 1600 W) and thermocouples are installed in the upper and lower tool halves to regulate the tool temperature.

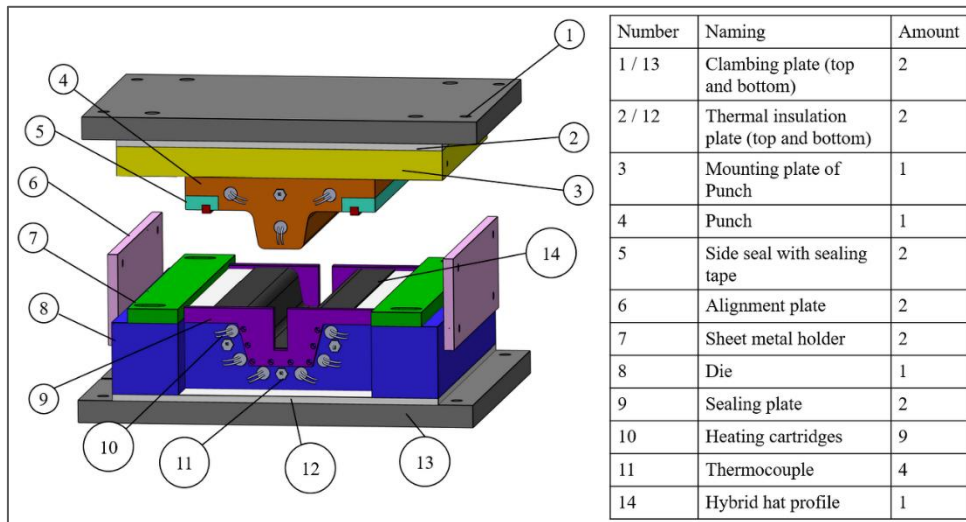


Figure 5: Pressing tool for manufacturing the hybrid hat profile

The purple plates on the front and back serve as a seal that prevents the epoxy from flowing out in this direction. The movement of the CFRP prepreg during the forming process presents a challenge for developing the seal along the profile length. Thus, it was assumed in this research that at the beginning of the forming phase, the flange area of the CFRP is not yet exposed to the pressing forces, so the risk of resin leakage is low. Only when the punch reaches the bottom dead centre does the CFRP prepreg in the flange area come into contact with the tool, and the resin begins to flow due to pressure and heat. Based on this, the concept of side sealing was developed. (Figure 6a) A groove was milled into the sealing block into which the sealing tape was inserted. The distance between the left and right sealing tape corresponds to the CAD model, precisely 170 mm. (see Figure 1)

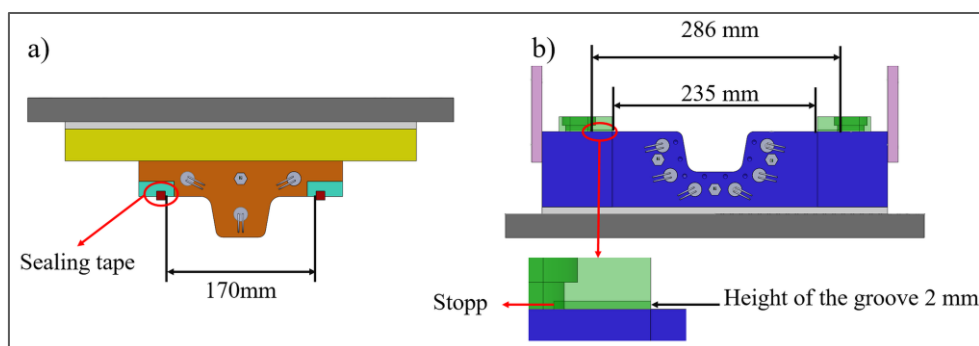


Figure 6: Illustration of the side sealing concept a) and b) the sheet holder

In conventional deep-drawing of a cup geometry, for example, a sheet holder is often used to counteract wrinkling due to the tangential compressive stress on the flange area [18]. In contrast, the shaping of the hat profile is merely a bending process, so there is no upsetting of the material in the flange area. Therefore, the sheet metal holders shown in green do not exert considerable force on the aluminium sheet but only prevent the sheet from tilting upwards during forming. The sheet holders have

a groove on the back with a 2 mm thickness (Figure 6b). Before forming, the left sheet holder is first placed on the lower die and lightly screwed. Then the aluminium sheet is inserted into the groove up to the marked stop, which aligns the sheet. Next, the right sheet holder can be placed on the sheet. After that, the two sheet metal holders were screwed tight with a defined torque.

3.5 Shear-edge test

In the context of this work, the adhesion properties of the hybrid hat profile were investigated using the shear-edge test, which, in contrast to the tensile shear test (German Standard DIN EN 1465), is characterized by its simple sample preparation. Furthermore, there is no bending moment during the test [19]. The specimen has a width of 25 mm and a height of 12.5 mm. (Figure 7b), similar to the overlap geometry in DIN EN 1465. The test setup shown in Figure 7a was installed in a universal testing machine from MTS Systems. During the test, the metal side of the sample is clamped in the fixture, and the CFRP side is pressed down by the shear edge so that a shear force can be generated at the boundary layer. The test speed was set at 5 mm/min.

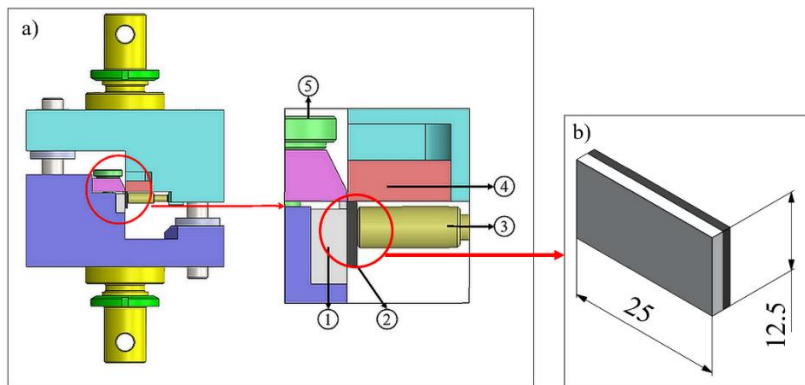


Figure 7: a) Testing device for shear-edge test. 1: Specimen holder aluminium side, 2: Specimen, 3: Clamping screw CFRP side, 4: Shear edge, 5: Clamping screw aluminium side, and b) specimen geometry

4 RESULTS AND DISCUSSION

4.1 Manufacturing of the hybrid hat profile

The aluminium sheet with a dimension of 286 mm*340 mm was firstly laser structured. For this, the laser direction of laser parameter 1 runs along both the X-direction (direction 1) and the Y-direction (direction 2) so that the influence of the laser direction can be examined. (Figure 8a) The next step was to cut and stack the CFRP prepregs. It was assumed that, unlike metal materials, the CFRP prepregs would not flow plastically. Thus, the initial length of the individual prepreg layers in the X-direction was determined from the CAD model, which is 235 mm. (Figure 8b, marked in green). The length in the Y-direction is similar to that of the aluminium sheet. While preparing the material, the pressing tool was heated simultaneously, the temperature of which was monitored by a heating regulator.

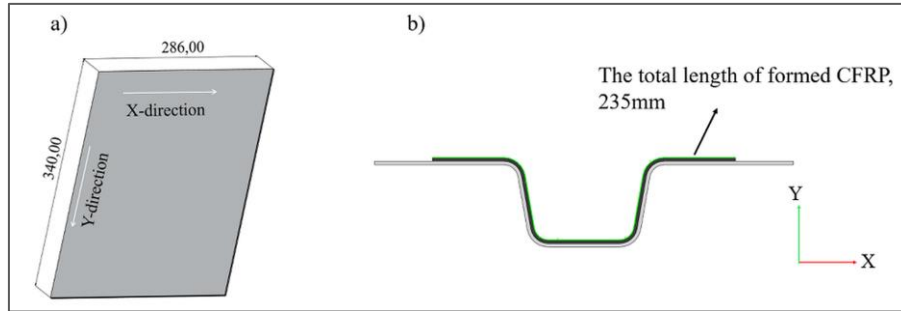


Figure 8: Geometry and laser direction of a) aluminium sheet, and b) initial length of CFRP prepreg in X-direction

Once the targeted temperature of 150°C is reached, the aluminium sheet can be placed on the tool as described in the previous section, followed by the placement of the stacked prepreg layers and the release foil, which prevents contamination of the tool. For positioning the stacked prepreg layers, the sheet holders here also serve as a stop, as the distance between the sheet holders is exactly 235 mm. (see Figure 6b). After this, the pressing process can take place. The punch first moves displacement controlled to the bottom dead centre to form the aluminium sheet. At this point, a forming force of approx. 90 kN was achieved, measured by a data acquisition system from HBM (further HBM, renamed in 2020). After that, the press switched to force-controlled mode. This way, the curing force (120 kN and 130 kN) can be maintained. After the curing process, which takes 5 min, the punch opens automatically to remove the component. Three compression springs in the die ensure easy removal of the hat profile. Finally, all hat profiles are post-cured in the oven at 180°C for 30 min

Figure 9a shows an example of a hat profile produced with laser parameter 1, direction 1. It can be seen that the geometry could be reproduced well without wrinkling. Moreover, no fibres are squeezed out in the front and back areas, and the fibres all run consistently in one direction. The slight deviation of the angle between the flange and frame area is due to the spring back from the aluminium sheet. (Figure 9b)

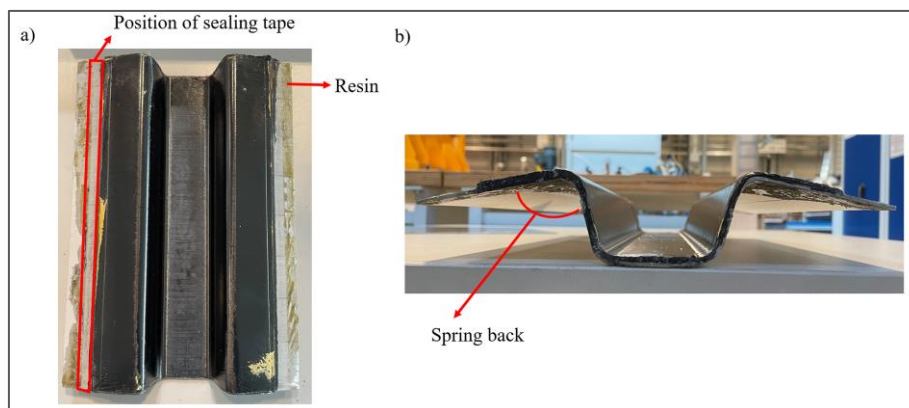


Figure 9: Illustration of the a) manufactured hat profile and b) the spring back effect of the aluminium sheet

Furthermore, the sealing tape on the side could almost avoid considerable resin leakage. Nevertheless, an amount of resin can still be seen. However, it should not be overlooked that there is a rectangular area on the aluminium sheet without resin. (Figure 9a) Therefore, it can be deduced that a small amount of resin could leak out just before contact between the sealing tape and the aluminium

sheet. As soon as the sealing tape is entirely in contact with the aluminium sheet and thus a sufficient sealing force can be generated by the further stroke movement of the punch, the seal works well.

4.2 Results shear-edge test

For the shear-edge tests, 5 specimens per parameter combination were cut from the flange, frame and bottom areas of the hat profile. Since the specimens from the frame area, mostly from laser parameter 3, already failed after the sample cutting and thus cannot provide valid results, they are not considered in the following. However, this could lead to the first conclusion that laser parameter 3 causes less adhesion improvement than other parameters. On the other hand, the poor adhesion properties could also be due to the lower pressing pressure in the frame area since the pressing force was determined vertically based on the projected surface.

The results from the flange and bottom area were then evaluated with a multifactorial analysis of variance (ANOVA) to investigate the influence of laser and manufacturing parameters (mainly pressing force). All results were checked in advance for normal distribution and variance homogeneity as a prerequisite [20]. Reference specimens with untreated aluminium sheets were not examined. Since it can be proven by numerous pieces of literature that laser pre-treatment can cause an improvement in the adhesion properties [21]. The ANOVA results are shown in the diagram below (Figure 10). The error bars in the graph indicate the confidence interval of the results. The confidence interval indicates that the actual mean value (here, the average shear strength) of a population has a 95% probability of falling within this range [20].

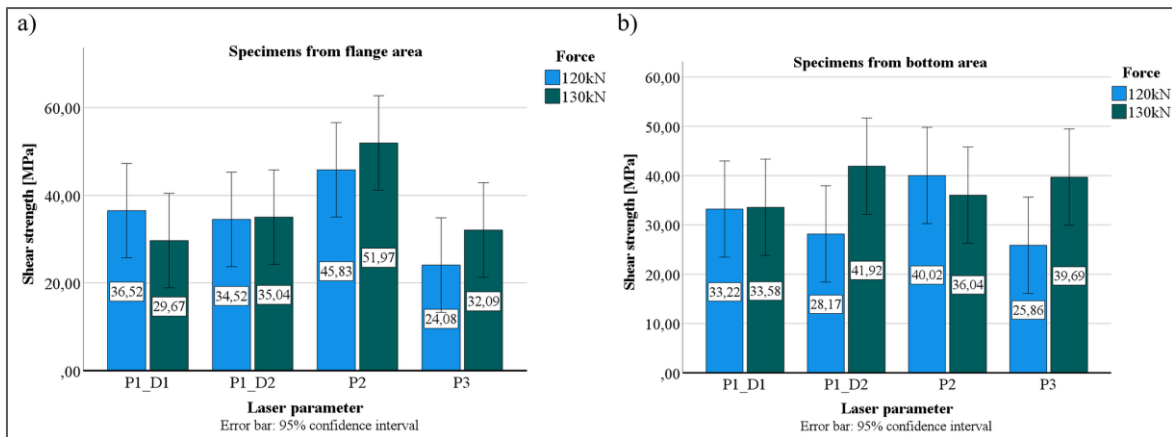


Figure 10: Shear strength of the specimens from a) flange and b) bottom area at different manufacturing parameters

The ANOVA analysis shows that the laser parameter plays an essential role for specimens from the flange area (Figure 10a), verified by the calculated P-value of 0.3 %. The P-value indicates whether the null hypothesis that the expected values (here, shear strength) of different groups do not differ can be rejected. The null hypothesis can be rejected if the P-value is less than 5 %. Thus, a significant difference in shear strength occurs when the laser parameter is changed in the flange area [22]. In contrast, an increase in the pressing force for the respective laser parameter has no significant influence on the shear strength, both in the flange area (P-value 60.5 %) and the bottom area (P-value 8.7 %).

The ANOVA results can also be recognised graphically. No statistically significant differences can be found between the groups if the confidence intervals overlap [20]. That is the case for parameters P1_D1 and P1_D2 in the flange area. In contrast, it can be seen from Figure 10a that the specimens with laser parameter 2 (P2) show a significantly higher shear strength compared to specimens with laser parameter 3 (P3) (P-value 4 %) at a pressing force of 120 kN. However, the average shear strength of specimens with laser parameter 2 is higher than those with laser parameter 1, laser direction 1 (P1_D1),

when the pressing force is 130 kN (P-value 3.3 %). Increasing the pressing force causes a deterioration of the results with laser parameter P1_D1, but an improvement with laser parameter P3 could be due to the laser structure.

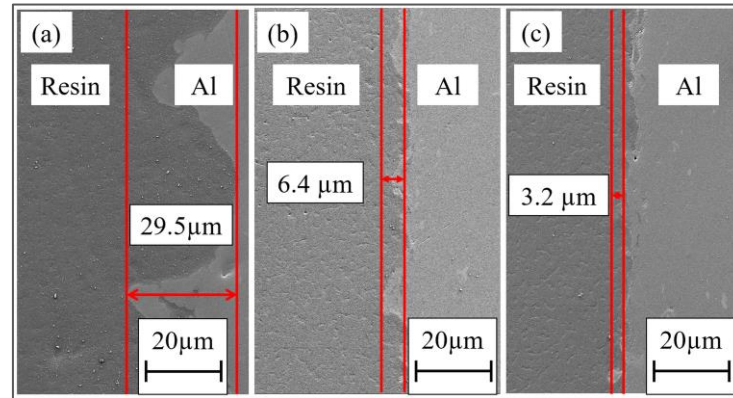


Figure 11: Wetting and bonding of the resin to the aluminium surfaces after laser pre-treatment with parameter (a) P1, (b) P2 and (c) P3

Figure 11 shows the cross-section of a single-lap joint specimen where two aluminium sheets were bonded with the epoxy resin. It can be seen that the crater height at P1 is significantly higher than that at P3. Therefore, the mechanical interlocking at P1 could be a main effect in improving the adhesion properties. However, these craters could be flattened at high forming force, negatively affecting the mechanical interlocking. In contrast, increasing the forming force could press more resin system into the laser structure at P3, resulting in better adhesion properties. Thus, it can be deduced from the ANOVA results that the structure height is not the only factor influencing the bonding properties, as the structure at P2 is lower than that at P1. Moreover, surface enlargement could also play a role, which should be investigated further.

Compared to the flange area, the average shear strength of the specimens from the bottom area (Figure 10b) does not differ significantly from each other when the laser parameter is changed. (P-value 69.8 %). A precise reason for this has not yet been found. But the high forming force could be mentioned as one reason, as the bottom area comes into contact with the punch first during the forming process and is thus exposed to high pressing force. As a result, the laser structure could be partially flattened for all parameters and no longer differ so much from each other.

5 CONCLUSION AND OUTLOOK

This paper provides an overview of the intrinsic manufacturing of hybrid components consisting of a laser-structured aluminium sheet of alloy AW-6082 in T6 condition and thermoset CFRP prepreg. For this purpose, a pressing tool was developed. The process temperature for all profiles is 150°C, and the curing time is 5 min. The main findings can be summarised as follows:

- A load-optimised layer structure was calculated using the FE method, which is 0°/45°/-45°/90°/90°/45°/-45°/0°.
- With the developed pressing tool and the sealing concept, the hybrid hat profile could be produced without much resin leakage and fibre squeezing-out. However, a spring back effect from the aluminium sheet can still be observed.
- Specimens for each parameter combination were cut from different profile areas (flange, bottom and frame). Their adhesion properties were investigated using the shear-edge test. The specimens from the frame area have the worst shear strength and partly fail after cutting, especially with laser parameter 3, which could be attributed to the laser structure on the one hand and to the lower pressing force in the frame area on the other hand.

- The average shear strength at the flange and bottom area was analysed using the ANOVA method. The results showed that the laser parameter significantly influences the average shear strength. Here, the parameter combination, 150 °C, 130 kN, 5 min and P2 achieve the highest shear strength of 51.97 MPa in the flange area. In contrast, no clear correlation could be found between the average shear strength and the laser parameter and the pressing force in the bottom area.

In summary, it can be stated that the developed pressing process can produce a hybrid hat profile with improved adhesion properties. Compared to some literature values, e.g. in [23] from Zinn, the hybrid plate specimen shows a best shear strength of only 31 MPa (tested by the shear-edge method), which consists of laser-structured aluminium and thermoset CFRP, produced with the Vacuum Assisted Resin Transfer Molding process (VARTM). The specimens with laser parameter 2 show a significantly higher shear strength within this publication. In addition, the manufacturing time (5 min) is also shorter compared to the VRTM process (approx. 45 min). Thus, the results within this work provide fundamental insights into the intrinsic manufacturing of metal-FRP hybrid components based on thermoset plastics. In the future, the influence of the manufacturing parameters, e.g. the pressing force, should be further investigated. Furthermore, the next step should be to evaluate the fracture surface of the samples using digital image analysis such as SEM to understand the adhesion mechanisms at the interface better.

ACKNOWLEDGEMENTS

This work was supported by the research project “Energy-efficient manufacturing and mechanism-based corrosion fatigue characterization of laserstructured hybrid structures“ (HA 5600/5-1, TR 373/9-1, WA 1672/65-1), funded by the Deutsche Forschungsgemeinschaft (DFG, German Research Foundation) – Project number - 426499947.

REFERENCES

- [1] B. Bader, E. Türck, T. Vietor, Multi material Design. A current overview of the used potential in automotive industries, *Proceedings of the 8rd Conference on Fascination hybrid lightweight construction, German: Faszination hybrider Leichtbau*, (Eds. K. Dröder, T. Vietor), Wolfsburg, Germany, May 29-30, 2018, Wolfsburger MobileLifeCampus, pp. 3–13 ([doi: https://doi.org/10.1007/978-3-662-58206-0](https://doi.org/10.1007/978-3-662-58206-0))
- [2] International Council on Clean Transportation, Europe’s CO2 emission performance standards for new passenger cars: Lessons from 2020 and future prospects - International Council on Clean Transportation, 2021+00:00. <https://theicct.org/publication/europes-co2-emission-performance-standards-for-new-passenger-cars-lessons-from-2020-and-future-prospects/> (accessed 4 April 2023.997Z).
- [3] Märkte/Unternehmen, *Lightweight Des*, 8, 2015, pp. 6–11 ([doi: https://doi.org/10.1007/s35725-015-0024-2](https://doi.org/10.1007/s35725-015-0024-2)).
- [4] T. Schnettke, P. Dreessen, K. Dröder, C. Vogler, D. Koch, T. Frey, B. Poller, A. Wedemeier, C. Vree, J. Kosowski, D. Riss, Film-adhesives for polymer-metal hybrid structures from laboratory to close-to-production, *Proceedings of the 8rd Conference on Fascination hybrid lightweight construction, German: Faszination hybrider Leichtbau*, (Eds. K. Dröder, T. Vietor), Wolfsburg, Germany, May 29-30, 2018, Wolfsburger MobileLifeCampus, pp. 157-166 ([doi: https://doi.org/10.1007/978-3-662-58206-0](https://doi.org/10.1007/978-3-662-58206-0)).
- [5] Z. Wang, C. Lauter, B. Sanitther, A. Camberg, T. Troester, Manufacturing and investigation of steel-CFRP hybrid pillar structures for automotive applications by intrinsic resin transfer moulding technology, *Int. J. Automotive Composites*, 2, 2016, pp. 229-242 ([doi: https://doi.org/10.1504/IJAUTO.2016.084322](https://doi.org/10.1504/IJAUTO.2016.084322)).
- [6] S.F. Koch, D. Barfuss, M. Bobbert, L. Groß, R. Grützner, M. Riemer, D. Stefaniak, Z. Wang, Intrinsic Hybrid Composites for Lightweight Structures: New Process Chain Approaches, *Advanced Materials Research*, 1140, 2016, pp. 239–246. ([doi:10.4028/www.scientific.net/AMR.1140.239](https://doi.org/10.4028/www.scientific.net/AMR.1140.239)).

- [7] B. Bernd-Arno, H. Sven, G. Nenad, M.-C. Moritz, W. Tim, N. André, Forming and Joining of Carbon-Fiber-Reinforced Thermoplastics and Sheet Metal in One Step, *Procedia Engineering*, 183, 2017, pp. 227–232 ([doi: https://doi.org/10.1016/j.proeng.2017.04.026](https://doi.org/10.1016/j.proeng.2017.04.026)).
- [8] B.-A. Behrens, S. Hübner, A. Neumann, Forming Sheets of Metal and Fibre-reinforced Plastics to Hybrid Parts in One Deep Drawing Process, *Procedia Engineering*, 81, 2014, pp. 1608–1613 ([doi: https://doi.org/10.1016/j.proeng.2014.10.198](https://doi.org/10.1016/j.proeng.2014.10.198)).
- [9] D. Trudel-Boucher, P. Kabala, J. Beuscher, M. Champagne, K. Dröder, Comparison of the Mechanical Properties of Adhesively Bonded and Mechanically Interlocked Steel/Fibre-Reinforced Thermoplastic Hybrids Produced Using One-Step Forming Process, *Proceedings of the Conference "Future Production of Hybrid Structures 2020"*, (Eds. K. Dröder, T. Vietor), Wolfsburg, Germany, May 27-28, pp. 211–219 ([doi: https://doi.org/10.1007/978-3-662-62924-6](https://doi.org/10.1007/978-3-662-62924-6)).
- [10] X. Fang, T. Kloska, Hybrid forming of sheet metals with long Fiber-reinforced thermoplastics (LFT) by a combined deep drawing and compression molding process, *Int. J of Material Forming*, 13, 2020, pp. 561–575 ([doi: https://doi.org/10.1007/s12289-019-01493-4](https://doi.org/10.1007/s12289-019-01493-4)).
- [11] J. Chen, K. Du, X. Chen, Y. Li, J. Huang, Y. Wu, C. Yang, X. Xia, Influence of surface microstructure on bonding strength of modified polypropylene/aluminum alloy direct adhesion, *Applied Surface Science*, 489, 2019, pp. 392–402 ([doi: https://doi.org/10.1016/j.apsusc.2019.05.270](https://doi.org/10.1016/j.apsusc.2019.05.270)).
- [12] J. Karger-Kocsis, *Polypropylene: An A-Z reference*, Kluwer Academic Publishers, The Netherlands, 1999.
- [13] G.W. Ehrenstein (Ed.), *Fibre composite plastics (German: Faserverbund-Kunststoffe: Werkstoffe - Verarbeitung - Eigenschaften)*, Hanser Publisher, Munich, 2006.
- [14] H. Lengsfeld, F. Wolff-Fabris, J. Krämer, J. Lacalle, V. Altstädt, *Fibre Composites: Prepregs and their processing (German: Faserverbundwerkstoffe: Prepregs und ihre Verarbeitung)*, Carl Hanser Publishers, Munich, 2015.
- [15] C. Lauter, M. Frantz, J.-P. Kohler, Crash tests of hybrid structures consisting of sheet metal and local CFRP reinforcements, *Conference paper of the 15th European Conference on Composite Materials, Venice, Italy, June 24-28, 2012*.
- [16] F. Rieg, R. Hackenschmidt, B. Alber-Laukant, *Finite Element Analysis for Engineers (German: Finite Elemente Analyse für Ingenieure)*, Carl Hanser Publishers, Munich, 2019.
- [17] A. Delp, J. Freund, S. Wu, R. Scholz, M. Löbbbecke, J. Haubrich, T. Tröster, F. Walther, Influence of laser-generated surface micro-structuring on the intrinsically bonded hybrid system CFRP-EN AW 6082-T6 on its corrosion properties, *Composite Structures*, 285, 2022 ([doi: https://doi.org/10.1016/j.compstruct.2022.115238](https://doi.org/10.1016/j.compstruct.2022.115238)).
- [18] H. Hoffmann, *Handbook Forming (German: Handbuch Umformen)*, Carl Hanser Publishers, Munich, 2012.
- [19] K.A. Weidenmann, L. Baumgärtner, B. Haspel, The Edge Shear Test - An Alternative Testing Method for the Determination of the Interlaminar Shear Strength in Composite Materials, *Materials Science Forum*, 825-826, 2015, pp. 806–813. ([doi: https://doi.org/10.4028/www.scientific.net/MSF.825-826.806](https://doi.org/10.4028/www.scientific.net/MSF.825-826.806)).
- [20] F. Huber, F. Meyer, M. Lenzen, *Basics of variance analysis (German: Grundlagen der Varianzanalyse)*, Springer Fachmedien Wiesbaden, Wiesbaden, 2014.
- [21] C. Zinn, M. Bobbert, C. Dammann, Z. Wang, T. Tröster, R. Mahnken, G. Meschut, M. Schaper, Shear strength and failure behaviour of laser nano-structured and conventionally pre-treated interfaces in intrinsically manufactured CFRP-steel hybrids, *Composites Part B: Engineering*, 151, 2018, pp. 173–185 ([doi: https://doi.org/10.1016/j.compositesb.2018.05.030](https://doi.org/10.1016/j.compositesb.2018.05.030)).
- [22] K. Siebertz, D. van Bebber, T. Hochkirchen, *Design of experiments (German: Statistische Versuchsplanung)*, Springer Publishers, Heidelberg, 2010.
- [23] C. Zinn, *Laser-induced nanostructuring of intrinsically manufactured hybrid structures: surface morphology, bonding and corrosion properties (German: Laserinduzierte Nanostrukturierung intrinsisch gefertigter Hybridstrukturen: Oberflächenmorphologie, Verbindungs- und Korrosionseigenschaften)*, Books on Demand, Norderstedt, 2019.